Paper No. 64—FE-9

On the Starting Characteristics of Supersonic Ejector Systems[1]

A. L. ADDY
Assistant Professor,
Department of Mechanical Engineering,
University of Illinois,
Urbana, Ill.

W. L. CHOW
Associate Professor,
Department of Mechanical Engineering,
University of Illinois,
Urbana, Ill.

The transient pumping characteristics of supersonic ejector systems are investigated both theoretically and experimentally. The theoretical analysis of this transient problem is based on quasi-steady flow concepts. The steady-state ejector analysis, upon which the present study must be based, considers the basic interaction between the primary and secondary streams as well as the viscous mixing effects which are the predominant flow mechanism at small secondary flow rates. The results of applying this steady-state analysis to the present problem are presented and shown to be in excellent agreement with experimentally observed ejector starting characteristics.

Introduction

High-altitude simulation for rocket-engine testing is often accomplished by employing the ejector action of the rocket-engine exhaust stream, Fig. 1, to lower the pressure in the secondary chamber and, hence, at the engine exit plane. In order to obtain meaningful steady-state test results in this manner, the characteristic time associated with the attainment of the final simulated conditions must be much less than the duration of the overall rocket-engine test. The present analysis is restricted to the aspects of the ejector action which eventually produces the final simulated high-altitude conditions.

For a given ejector configuration the minimum simulated pressure occurs when the secondary flow rate is zero as a consequence of the primary stream expanding and subsequently attaching to the diffuser wall. This minimum simulated pressure, which is equal to the pressure of the fluid in the wake thus formed, is generally termed as the internal base pressure. It has been well established [2–5][2] that the internal base pressure problem is characterized by the viscous mixing between the primary stream and the fluid entrained in the wake and the recompression which occurs near the reattachment point. Since this flow condition is maintained by the viscous mixing effects, it is expected that this mixing would also play a dominant role in its establishment.

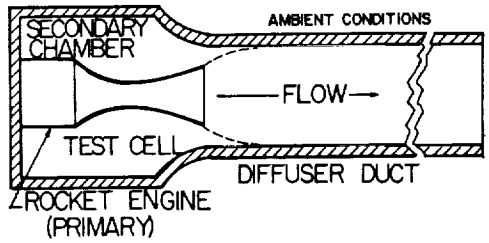

Fig. 1 Typical altitude-simulation system for rocket-engine testing

Ihrig and Korst [6] have shown in a recent investigation of the adjustment of separated flow regions subject to transient external flow conditions that the characteristic times associated with adjustment of transport quantities are much larger than the characteristic time required for adjustments resulting from pressure waves. Such conclusions encouraged the study of the present problem on a quasi-steady basis; namely, that the pumping characteristics at any instant can be described by the corresponding steady-state ejector performance.

A survey of previous analyses [7–11] of steady-state ejector systems indicated that these treatments (e.g., by Fabri, et al. [9–11]) cannot be adopted for the present study since the viscous effects were completely ignored. A more comprehensive analysis, including the viscous effects, of steady-state supersonic ejector systems was developed by the authors.

In this paper, the prediction of the starting characteristics em-

[1] This paper is based on the PhD thesis, reference [1], by A. L. Addy.

[2] Numbers in brackets designate References at end of paper.

Contributed by the Fluid Mechanics Subcommittee, Fluids Engineering Division, for presentation at the Fluids Engineering Conference, Philadelphia, Pa., May 18–21, 1964, of The American Society of Mechanical Engineers. Manuscript received at ASME Headquarters, February 20, 1964. Paper No. 64—FE-9.

Nomenclature

A = area

$C = \dfrac{u}{u_{max}} = \left(1 + \dfrac{2}{k-1}\dfrac{1}{M^2}\right)^{-1/2}$, Crocco number

D = diameter

k, k = c_p/c_v, ratio of specific heats

L = length of cylindrical tube

M = Mach number

$M^* = \left(\dfrac{k+1}{2}M^2/1 + \dfrac{k-1}{2}M^2\right)^{1/2}$

P = absolute pressure

P_a = ambient pressure, see Fig. 2

R = radius, or gas constant

T = absolute temperature

t = time, or thickness of primary nozzle base

l = dimensionless time (see text for definition)

u = velocity component in the x-direction

V = velocity or secondary volume (V_s)

v_b = velocity component of secondary fluid in y-direction at large negative value of η

W = mass rate of flow

x, y = coordinates in intrinsic coordinate system

X, Y = coordinates in reference coordinate system

Z = abscissa of coordinate system

$\eta = \sigma\dfrac{y}{x}$, dimensionless coordinate

η_m = dimensionless shift of intrinsic coordinate system x, y with respect to reference coordinate system X, Y

$\alpha = \tan^{-1}[1/(M^2-1)^{1/2}]$, Mach angle

θ = streamline angle

ρ = density

σ = similarity parameter for homogeneous coordinate y/x

$\varphi = u/u_a$, dimensionless velocity

$\Lambda = T_0/T_{0a}$, stagnation temperature ratio

$\dfrac{-\sigma_{11}\delta^*}{x_M}$ = dimensionless displacement thickness for jet-mixing region

$\zeta(t)$ = instantaneous secondary-to-primary stagnation pressure ratio, $P_{0s}(t)/P_{0p}$

τ = dimensionless time, t/l

(Continued on next page)

ploying the recently established steady-state analysis is presented. In addition, the starting and steady-state ejector characteristics are compared with experimental results.

Transient Analysis

For the ejector geometry shown in Fig. 1, the objective of this analysis is to establish the secondary stagnation pressure (P_{0s}) as a function of time after the primary flow is established and maintained at a constant value. The analysis is restricted to those cases where the ambient-to-primary stagnation pressure ratio (P_a/P_{0p}) is less than or equal to the value $(P_a/P_{0p})_s$ which is just required to reduce the steady-state secondary stagnation pressure ratio (P_{0s}/P_{0p}) to the internal base pressure ratio for the given geometry.[3] In addition, the primary and secondary fluids are assumed to have the same composition and to obey the equation of state, $P = \rho RT$.

If the fluid in the secondary volume is assumed to be of uniform density $\rho_{0s}(t)$ at each instant, the continuity equation in nonsteady form is

$$\frac{\partial}{\partial t}\int_{V_s} \rho_{0s}(t)dV = -W_s(t) \tag{1}$$

where $W_s(t)$ is the instantaneous secondary flow rate. Assuming that the secondary fluid expands isentropically so as to occupy the volume completely, equation (1) can be written as

$$W_s(t) = \frac{-V_s}{kRT_{0s,0}}\left[\frac{P_{0s}(t)}{P_{0s,0}}\right]^{\frac{1-k}{k}}\frac{dP_{0s}(t)}{dt} \tag{2}$$

where the subscript 0 denotes the initial value of the secondary variables.

The primary-flow rate can be used to obtain a convenient nondimensional form of equation (2). It is

$$\frac{W_s(t)}{W_p}\left[\frac{T_{0s,0}}{T_{0p}}\right]^{1/2} = -\zeta^{\frac{1-k}{k}}\,(d\zeta/d(t/G)) \tag{3}$$

where, for convenience, the constant G and the dependent variable $\zeta(t)$ are defined as

$$G = \frac{1}{k}\left[\frac{k+1}{2}\right]^{\frac{k+1}{2(k-1)}}\left[\frac{V_s}{A_p^*(kg_cRT_{0s,0})^{1/2}}\right]\left[\frac{P_{0s,0}}{P_{0p}}\right]^{\frac{k-1}{k}} \tag{4}$$

and

$$\zeta(t) = P_{0s}(t)/P_{0p} \tag{5}$$

[3] The ambient-to-primary pressure ratio $(P_a/P_{0p})_s$, defined in [12, 13] as the "starting" pressure ratio, can be estimated reasonably well for certain geometries [2]. An empirical relationship for calculating this starting pressure ratio has also been developed in [12, 13].

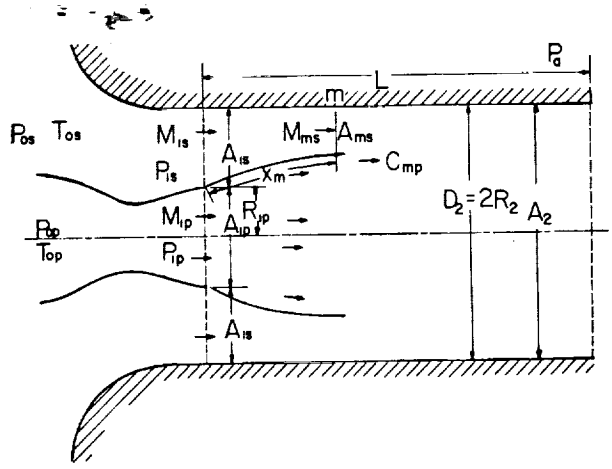

Fig. 2 Flow model for ejector systems

Based on the quasi-steady flow concept, the mass-flow ratio from equation (3) can be expressed functionally as

$$\frac{W_s}{W_p}\left[\frac{T_{0s}}{T_{0p}}\right]^{1/2} = F(\zeta) \tag{6}$$

The functional relationship between the mass-flow ratio and the instantaneous stagnation pressure ratio must be determined from the steady-state ejector characteristics. On this basis, a form of equation (3) which is more amendable to numerical calculation is

$$(t - t_0)/G = -\int_{\zeta_0}^{\zeta}\frac{\zeta^{\frac{1-k}{k}}\,d\zeta}{\left[\frac{W_s}{W_p}\left(\frac{T_{0s,0}}{T_{0p}}\right)^{1/2}\right]} \tag{7}$$

where t_0 and ζ_0 are reference initial conditions.

The functional relationship given by equation (6) will now be established from the steady-state analysis of the ejector pumping characteristics. After this relationship has been established, the secondary stagnation pressure ratio, $\zeta = P_{0s}/P_{0p}$, can then be easily determined as a function of time from equation (7) for given values of the initial conditions.

Steady-State Analysis[4]

The ejector configuration to be studied, along with the associated notation, is shown in Fig. 2. For simplicity, the essential

[4] A more detailed analysis of the steady-state ejector operating characteristics is presented in [1] and a paper submitted by the authors to the *AIAA Journal* entitled, "On the Interaction Between the Primary and the Secondary Streams of Supersonic Ejector Systems and Their Performance Characteristics," submitted May, 1963, and revised November, 1963. Accepted for publication, February, 1964.

Nomenclature

Subscripts

0 = stagnation condition or initial condition
1 = section 1
2 = section 2
4 = state downstream of oblique shock, see Fig. 7
a = refers to primary stream within two-stream mixing region, to free-stream adjacent to mixing region, or ambient conditions into which diffuser duct is exhausting
b = secondary stream within two-stream mixing region
d = discriminating streamline
e = exit section of ejector system
i = inviscid flow
j = jet-boundary streamline
l = limiting initial secondary-flow Mach number
m = states of fluids when secondary flow has a minimum flow area
M = mixing region; e.g., x_M = length along mixing region
p = primary stream
s = secondary stream or value of pressure ratio required to just attain base pressure for a given geometry
w = shroud wall
n, n', q = points in inviscid flow fields, see Fig. 5
η_{Ra}, η_{Rb} = large positive and negative values of η, see text
I = jet mixing of one stream with a quiescent wake
II = two-stream jet mixing

Functions and Integrals

$$f(\mathbf{M}) = \left(\frac{kg_c}{R}\right)^{1/2}\mathbf{M}\left(1 + \frac{k-1}{2}\mathbf{M}^2\right)^{1/2}$$

$$A/A^* = \frac{1}{\mathbf{M}}\left[\frac{2}{k+1}\times\left(1 + \frac{k-1}{2}\mathbf{M}^2\right)\right]^{\frac{k+1}{2(k-1)}}$$

$I_1(\eta) = I_1\left(\frac{T_{0b}}{T_{0a}}, C_a^2, \varphi_b, \eta\right)$, see definition in text

$I_2(\eta) = I_2\left(\frac{T_{0b}}{T_{0a}}, C_a^2, \varphi_b, \eta\right)$, see definition in text

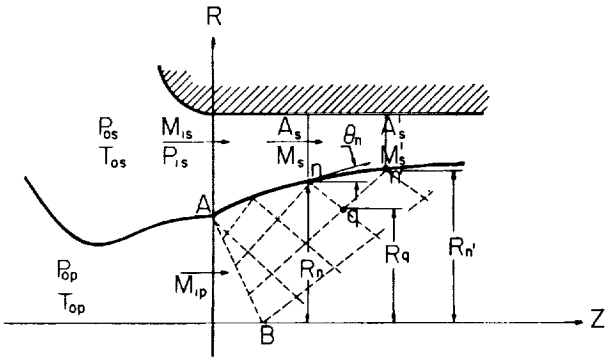

Fig. 3 Two-stream, inviscid, interacting flow model

geometric characteristics of this system are an axisymmetric primary nozzle which produces uniform supersonic flow at the nozzle exit,[5] a cylindrical constant-area shroud, and a secondary-stream entrance section which establishes at Section 1 the minimum geometrical flow area.

Steady-state ejector operation, depending upon the relative level of the ambient to primary pressure ratio (P_a/P_{0p}), can be divided into two flow regimes. These flow regimes are determined according to whether the upstream flow conditions are independent of the pressure ratio (P_a/P_{0p}) or dependent on it. These flow regimes will now be analyzed.

Upstream Flow Conditions Independent of Ambient-to-Primary Pressure Ratio

For certain values of the primary and secondary stagnation pressures, the secondary stream will attain sonic flow conditions at Section 1.[6] The secondary flow will remain choked at Section 1 until the value of P_{0s}/P_{0p} is reduced so that the secondary flow attains sonic conditions somewhere downstream of Section 1 as a result of the mutual interaction between the primary and secondary streams.[7] Further reduction of the stagnation pressure ratio, P_{0s}/P_{0p}, will cause the primary jet boundary to be first tangent and then to impinge on the shroud wall until the minimum pressure ratio (the internal base pressure ratio) is reached. In the vicinity of small secondary flow rates, it has been recognized that the viscous effects are the dominating flow mechanism [2–5].

"Saturated Supersonic" Flow Regime. Since the secondary flow is choked at Section 1, the mass-flow characteristics for this regime are readily established [14] as

$$\left[\frac{W_s}{W_p}\left(\frac{T_{0s}}{T_{0p}}\right)^{1/2}\right]_{M_{1s}=1} = \frac{A_{1s}}{A_p^*}\cdot\frac{P_{0s}}{P_{0p}} \tag{8}$$

"Supersonic" Flow Regime. For this flow regime, the choking point is now located in the downstream region, e.g., at the point m, Fig. 2. If the mixing along the boundary of the primary and secondary streams up to m is considered to be a secondary effect in the sense of boundary-layer concepts, the flow field between Section 1 and the choking location can be determined from the mutual interaction between the "corresponding inviscid secondary and primary streams." After the flow field has been determined from the inviscid interaction, the effects of mixing can then be accounted for by superimposing the mixing region on the inviscid solution.

Inviscid Two-Stream Interaction. The inviscid-flow model consists of the uniform secondary stream interacting with the expanding primary stream, Fig. 3. The secondary stream is considered to be one-dimensional in nature while the primary stream is treated by the method of characteristics. The requirements of this flow model are that the streams coexist in the available flow area, that the pressure across the boundary of the streams must be continuous, and that the secondary flow area must be minimum at the location where $\mathbf{M}_s = 1$, e.g., at m

$$\left[\frac{dA_s}{dZ}\right]_m = 0 \quad \text{when} \quad \mathbf{M}_{sm} = 1 \tag{9}$$

For a chosen pair of values of $\mathbf{M}_{1s}$ and $P_{1s}/P_{0p}(<P_{1p}/P_{0p})$[8] the primary fluid will undergo a Prandtl-Meyer expansion at the corner, and the primary flow field may be calculated by repeated "field point" calculations. For the calculation of the boundary points, which requires consideration of the secondary flow field, one assumes that the boundary point n and the field point q, Fig. 3, have been established by previous calculations. Then for the unknown boundary point n', $Z_{n'}$, and $R_{n'}$, may be found from the relations

$$(R_{n'} - R_n) = (Z_{n'} - Z_n)\tan\theta_{nn'} \tag{10}[9]$$

and

$$(R_{n'} - R_q) = (Z_{n'} - Z_q)\tan(\theta + \alpha)_{qn'} \tag{11}$$

The condition of coexistence in the available area yields the relationship for $\mathbf{M}_s'$:

$$\frac{A}{A^*}(\mathbf{M}_s') = \frac{(R_2^2 - R_{n'}^2)}{(R_2^2 - R_{1p}^2)}\cdot\frac{A}{A^*}(\mathbf{M}_{1s}) \tag{12}$$

where $A/A^*(\mathbf{M})$ is the one-dimensional area function [14]. The requirement of continuity of pressure across the boundary gives, for the point n', the relationship between Mach numbers $\mathbf{M}_{pn'}$ and $\mathbf{M}_s'$

$$\frac{P}{P_{0p}}(\mathbf{M}_{pn'}) = \frac{P}{P_{0s}}(\mathbf{M}_s')\left[(P_{1s}/P_{0p})\Big/\frac{P}{P_{0s}}(\mathbf{M}_{1s})\right] \tag{13}$$

where

$$\frac{P}{P_0}(\mathbf{M}) = \left[1 + \frac{k-1}{2}\mathbf{M}^2\right]^{-k/(k-1)}$$

From the characteristic relation,

$$(\theta_{n'} - \theta_q) - \frac{(\mathbf{M}_{Pn'}^* - \mathbf{M}_q^*)}{(\mathbf{M}^*\tan\alpha)_{qn'}} + \left[\frac{1}{R}\frac{\tan\theta\tan\alpha}{(\tan\theta + \tan\alpha)}\right]_{qn'}(R_{n'} - R_q) = 0 \tag{14}$$

the streamline angle of the primary fluid, $\theta_{n'}$, can be found.

The flow-field calculations are continued until a minimum secondary-flow area is established; the criterion for such a minimum area is

$$\frac{dR_p}{dZ} = \frac{R_w(Z)}{R_p(Z)}\cdot\frac{dR_w(Z)}{dZ} \tag{15a}$$

which for the present case becomes

$$\frac{dR_p}{dZ} = 0 \quad \text{since} \quad \frac{dR_w(Z)}{dZ} \equiv 0 \tag{15b}$$

In general, the secondary-flow Mach number at this minimum area will be less than one if the initially selected value of $\mathbf{M}_{1s}$ is small; hence by gradually increasing the value of $\mathbf{M}_{1s}$, for the same P_{1s}/P_{0p}, one will eventually obtain sonic flow conditions at the minimum secondary-flow area. This value of $\mathbf{M}_{1s}$ is defined as the "limiting" inviscid initial Mach number $\mathbf{M}_{1sl,i}$. For the values of $\mathbf{M}_{1sl,i}$ and P_{1s}/P_{0p}, the "limiting" inviscid mass-flow ratio is given by

[5] The nozzle is assumed always to flow full.

[6] Termed by Fabri, et al., as the "saturated supersonic" flow regime [9, 10, 11].

[7] Termed by Fabri, et al., as the "supersonic" flow regime [9, 10, 11].

[8] $\mathbf{M}_{1s}$ and P_{1s}/P_{0p} were chosen as independent variables to facilitate the calculations.

[9] The double subscript notation implies that the average values of the variables are to be used.

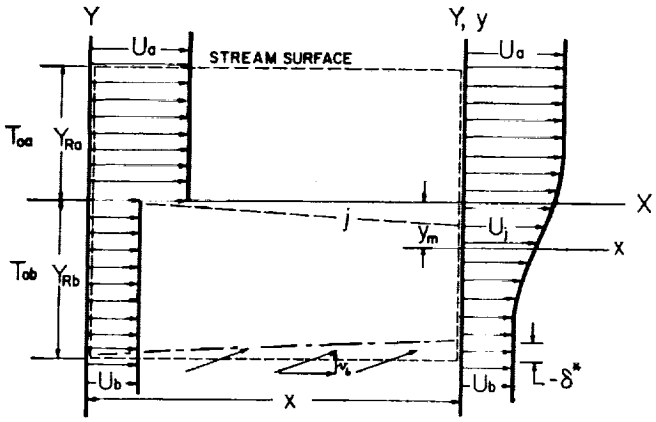

Fig. 4 Flow model for constant-pressure jet mixing between two streams

$$\left[\left(\frac{T_{0s}}{T_{0p}}\right)^{1/2}\frac{W_s}{W_p}\right]_{I,i} = \frac{A_{1s}}{A_{1p}}\cdot\frac{[P_{1s}/P_{0p}]}{[P_{1p}/P_{0p}]}\cdot\frac{f(\mathbf{M}_{1sI,i})}{f(\mathbf{M}_{1p})} \qquad (16)$$

where $f(\mathbf{M})$ is the mass flow function

$$f(\mathbf{M}) = \left[\frac{kg_c}{R}\left(1 + \frac{k-1}{2}\mathbf{M}^2\right)\right]^{1/2}\mathbf{M}$$

In addition to the inviscid mass-flow ratio, detailed information concerning the flow field is obtained, e.g., the pressure distribution along the shroud and the local flow properties along the non-constant pressure boundary between the streams.

It should be pointed out that the calculations follow typical step-by-step iterative procedures which can only be performed by a high-speed digital computer. The calculations for the present study were carried out on Illiac.[10]

Two-Stream Viscous Mixing. For the present problem, the mixing actually takes place along a non-constant pressure boundary. However, the assumption is made here that the viscous effects, between the two compressible streams, may be evaluated on the basis of quasi-constant-pressure turbulent jet mixing. This method approximates the actual velocity profile, at a given section, by the velocity profile which would result if the two streams, based on local flow conditions at this section, were mixed at constant pressure [15].[11]

It has been established for fully developed turbulent jet-mixing regions that the velocity profiles are similar for the homogeneous coordinate $\eta = \sigma y/x$ where σ is a similarity parameter [16, 19]. The velocity profile for the two-stream fully developed turbulent jet-mixing region is given by [17]

$$\varphi(\eta) = \frac{u}{u_a} = \left[\frac{1+\varphi_b}{2} + \frac{1-\varphi_b}{2}\,\mathrm{erf}\,(\eta)\right] \qquad (17)$$

where $\varphi_b = u_b/u_a$.

This profile is assumed to hold for a coordinate system x, y that is essentially displaced from the physical coordinate system X, Y, Fig. 4, by an amount y_m, i.e.,

$$x \approx X$$

and $y \approx Y + y_m(x)$ with $y_m(0) = 0$. The value of y_m must then be determined by the application of the continuity and momentum-integral relations to the control volume in Fig. 4. As a result of this analysis, y_m expressed in dimensionless form as η_m is given by

$$\eta_m = \eta_{Ra} - \frac{1}{(1-\varphi_b)}\left[I_2(\eta_{Ra}) - \varphi_b I_1(\eta_{Ra})\right] \qquad (18)$$

[10] Electronic digital computer, University of Illinois.

[11] This analysis is an extension of the previous study of mixing between a single stream and a quiescent wake which has been widely adopted for separated-flow studies [16].

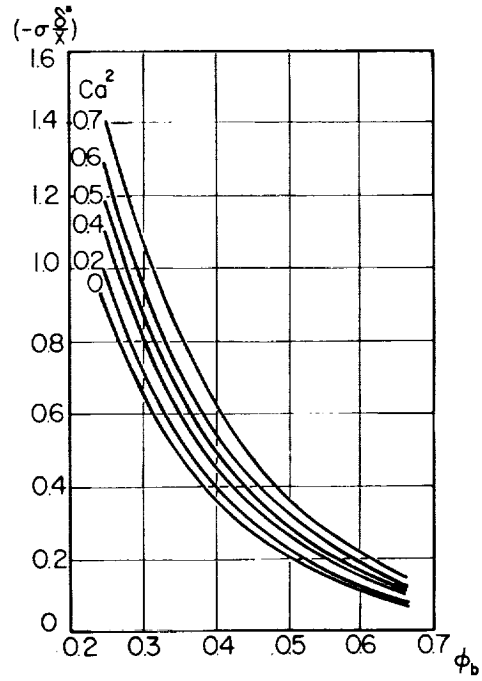

Fig. 5 Dimensionless displacement thickness for two-stream mixing regions

where $I_1(\eta)$, $I_2(\eta)$ are the short notation for the integrals

$$I_1\left(\frac{T_{0b}}{T_{0a}}, C_a^2, \varphi_b, \eta\right) = \frac{(1-C_a^2)\varphi_b\eta_{Rb}}{(T_{0b}/T_{0a} - C_a^2\varphi_b^2)} + \int_{\eta_{Rb}}^{\eta}\frac{(1-C_a^2)\varphi}{(\Lambda - C_a^2\varphi^2)}\,d\eta \qquad (19a)$$

and

$$I_2\left(\frac{T_{0b}}{T_{0a}}, C_a^2, \varphi_b, \eta\right) = \frac{(1-C_a^2)\varphi_b^2\eta_{Rb}}{(T_{0b}/T_{0a} - C_a^2\varphi_b^2)} + \int_{\eta_{Rb}}^{\eta}\frac{(1-C_a^2)\varphi^2}{(\Lambda - C_a^2\varphi^2)}\,d\eta \qquad (19b)$$

$\Lambda(\eta)$, the stagnation-temperature profile, is given by the Crocco integral relationship for fluids of unity turbulent Prandtl number as

$$\Lambda(\eta) = \frac{T_0}{T_{0a}} = \frac{1}{(1-\varphi_b)}\left[\left(\frac{T_{0b}}{T_{0a}} - \varphi_b\right) + \left(1 - \frac{T_{0b}}{T_{0a}}\right)\varphi\right] \qquad (20)$$

η_{Ra} and η_{Rb} are, respectively, positive and negative values of η such that

$$(1 - \varphi(\eta_{Ra})) < \epsilon_1, \qquad |1 - \Lambda(\eta_{Ra})| < \epsilon_2$$

and

$$(\varphi(\eta_{Rb}) - \varphi_b) < \epsilon_3, \qquad \left|\frac{T_{0b}}{T_{0a}} - \Lambda(\eta_{Rb})\right| < \epsilon_4$$

where ϵ_1, ϵ_2, ϵ_3, and ϵ_4 are arbitrarily small positive quantities.

It can be shown that the "jet boundary streamline," j, which separates the two streams, will satisfy the relationship

$$I_1(\eta_j) = [I_1(\eta_{Ra}) - I_2(\eta_{Ra})]/(1-\varphi_b) \qquad (21)$$

A displacement thickness, δ^*, due to the mixing between the streams can be defined, for convenience, as (Fig. 4)

$$\delta^* = -\frac{v_b}{u_b}x_M$$

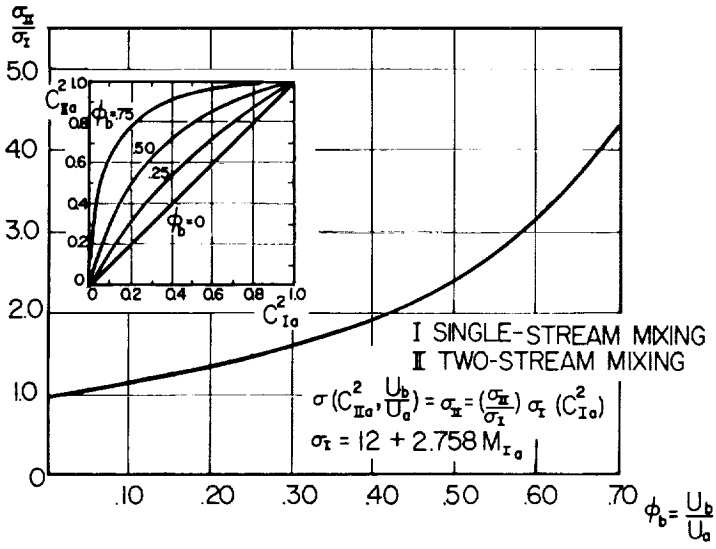

Fig. 6 Similarity parameter σ_{II}, for the two-stream mixing region

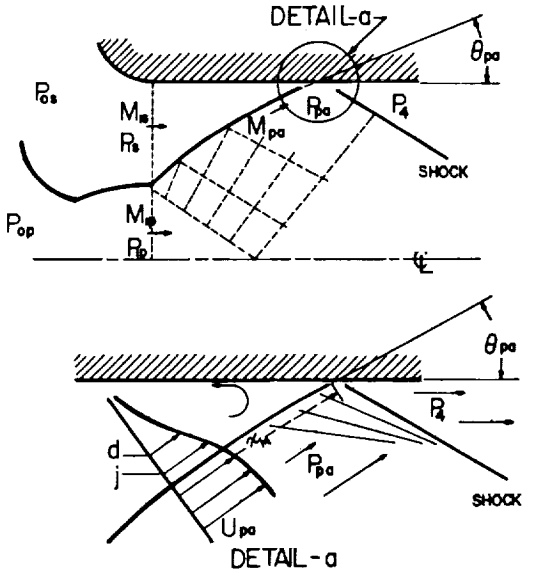

Fig. 7 Flow model within Region I (small secondary-flow rates)

This displacement thickness can be evaluated in dimensionless form by

$$\frac{-\sigma_{II}\delta^*}{x} = \frac{\left(\frac{T_{0b}}{T_{0a}} - C_a^2\varphi_b^2\right)}{\varphi_b(1 - C_a^2)}\,[I_1(\eta_j)] - \eta_m \qquad (22)$$

where σ_{II} is the two-stream similarity parameter. For the present analysis where $\Lambda \equiv 1$ (isoenergetic mixing), the dimensionless displacement thickness has been evaluated and presented in Fig. 5 for various values of the parameter C_a^2. The numerical results of a rational consideration [17] of σ_{II} are plotted in Fig. 6.

This mixing region is superimposed on the already calculated inviscid-flow field, and the effect of the mixing will result in an increase in the secondary-flow rate which is given in dimensionless form by

$$\left[\frac{\Delta W_s}{W_p}\right]_M \doteq \frac{2}{\sigma_{II}}\cdot\frac{A}{A^*}(\mathbf{M}_{1p})\cdot\frac{R_M}{R_{1p}}\cdot\frac{x_M}{R_{1p}}\cdot\frac{P_{0s}}{P_{0p}}\cdot\left[-\frac{\sigma_{II}\delta^*}{x_M}\right] \qquad (23)$$

where $\Delta W_s/W_p$ is to be evaluated using the stream properties at the section where the secondary flow is choked.

The limiting initial secondary-flow Mach number $\mathbf{M}_{1sl}$ (with the viscous effects included) can now be found through the relation

$$f(\mathbf{M}_{1sl}) = \frac{A_{1p}}{A_{1s}}\cdot\frac{P/P_{0p}(\mathbf{M}_{1p})}{P_{1s}/P_{0p}}\cdot f(\mathbf{M}_{1p})\left[\left(\frac{W_s}{W_p}\right)_i + \left(\frac{\Delta W_s}{W_p}\right)_M\right] \qquad (24)$$

The foregoing analysis can be used to determine the ejector-flow characteristics within the supersonic regime as long as the primary jet boundary does not impinge on the shroud wall (defined here as Region II) and the two-stream, inviscid-flow field is not significantly modified by the mixing.

At low values of P_{1s}/P_{0p}, which correspond to low secondary-flow rates, the secondary fluid entering at Section 1 will be completely entrained while it is interacting and mixing with the primary stream so that the primary jet boundary will impinge on the shroud wall, Fig. 7. Near the impingement point, an oblique shock wave exists which creates a region of high static pressure immediately downstream of the impingement point. For the recompression, the strength of this shock is determined from the plane two-dimensional oblique shock relation

$$\frac{P_4}{P_{pa}} = \frac{P_4}{P_{pa}}(\mathbf{M}_{pa}, \theta_{pa}) \qquad (25)$$

where $\mathbf{M}_{pa}$ and θ_{pa} are the Mach number and the streamline angle of the primary stream in the vicinity of the impingement point, Fig. 7. The values of $\mathbf{M}_{pa}$ and θ_{pa} are obtained from the inviscid interacting-flow field calculations for small selected values of P_{1s}/P_{0p} and $\mathbf{M}_{1s}$.

A "discriminating" streamline d, Fig. 7, can be defined within the single-stream jet-mixing region ($\varphi_b = 0$) as the streamline which has just sufficient mechanical energy to penetrate into the region of high static pressure downstream of the impingement point through a complete isentropic (although irreversible diabatic) recompression.[12] Hence, it divides the entrained fluid which has sufficient mechanical energy to "escape" from the wake and the fluid which remains in the wake. The "discriminating streamline" can be determined from the relationship

$$\frac{P_4}{P_{pa}} = \frac{P_{0d}}{P_d} = \left[1 - \frac{k-1}{k+1}\mathbf{M}_d^{*2}\right]^{-\left(\frac{k}{k-1}\right)} \qquad (26)$$

The secondary flow which "escapes" into this high-pressure region is then given by

$$W_s \doteq 2\pi R_2 \int_{y_d}^{y_j} \rho u\,dy \qquad (27)$$

where j is the "jet-boundary streamline" and d is the "discriminating streamline" within the mixing region with $\varphi_b = 0$, Fig. 7. Equation (27) can be reduced to the dimensionless form ($\varphi_b = 0$)

$$\left[\frac{W_s}{W_p}\right]_M = \frac{2}{\sigma_1}\cdot\frac{R_2}{R_{1p}}\cdot\frac{x_M}{R_{1p}}\cdot\frac{A/A^*(\mathbf{M}_{1p})}{A/A^*(\mathbf{M}_{pa})}\,[I_1(\eta_j) - I_1(\eta_d)] \qquad (28)$$

where σ_1 is the single-stream mixing parameter.

Since small values of $\mathbf{M}_{1s}$ and P_{1s}/P_{0p} were selected in order to determine the inviscid interacting flow field, continuity of the secondary fluid requires that the solution value of $\mathbf{M}_{1s}$, namely, $\mathbf{M}_{1sl}$, must satisfy the relationship

$$\left[\frac{W_s}{W_p}\right]_M = \frac{A_{1s}}{A_{1p}}\cdot\frac{(P_{1s}/P_{0p})}{P/P_{0p}(\mathbf{M}_{1p})}\cdot\frac{f(\mathbf{M}_{1sl})}{f(\mathbf{M}_{1p})} \qquad (29)$$

The value of $\mathbf{M}_{1sl}$ must then be found by a trial-and-error procedure for each selected value of P_{1s}/P_{0p} until equation (29) is satisfied.

The mass-flow characteristics for this flow regime (termed here

[12] This concept is termed as the "escape criterion" [2, 3].

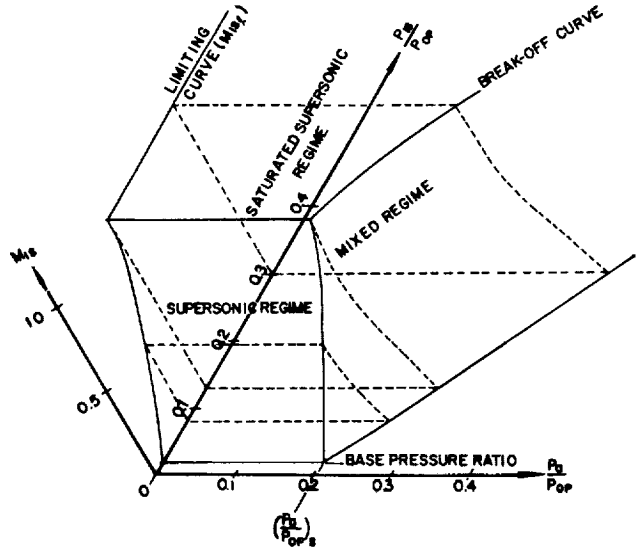

Fig. 8 Typical solution surface for steady-state ejector systems (M_{1s} versus P_{1s}/P_{0p} and P_a/P_{0p})

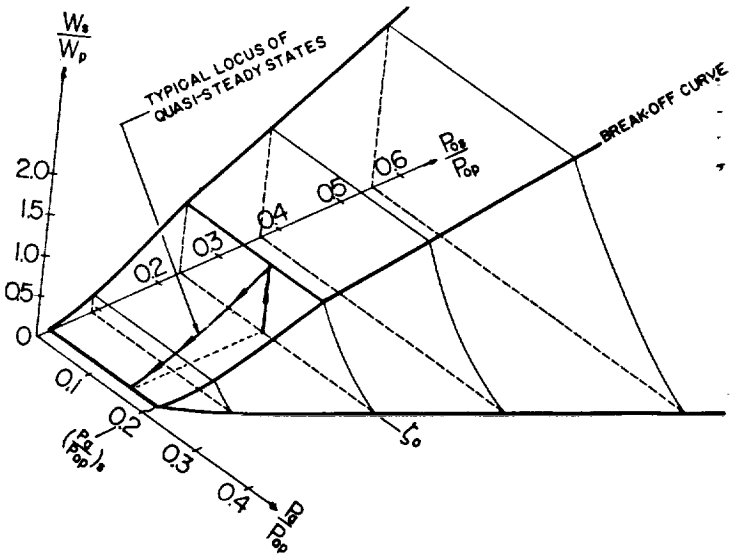

Fig. 9 Typical mass-flow characteristics for an ejector system (W_s/W_p versus P_{0s}/P_{0p} and P_a/P_{0p})

Region I) are established by calculating M_{1sl} for various values of P_{1s}/P_{0p} which will join smoothly with Region II.[13] For the limiting case, the internal base pressure solution will be obtained, $M_{1sl} = 0$, for which the primary stream boundary is a constant-pressure boundary and the j and d-streamlines coincide. Thus, the ejector steady-flow characteristics can be established by the foregoing calculation method, in the functional form

$$M_{1sl} = M_{1sl}(P_{1s}/P_{0p}) \tag{30}$$

and

$$\frac{W_s}{W_p} = \frac{W_s}{W_p}(P_{0s}/P_{0p}) \tag{31}$$

for the flow regime where the upstream flow conditions are independent of P_a/P_{0p}.

Flow Conditions Dependent on Ambient-to-Primary Pressure Ratio

As was pointed out by Fabri [11], the secondary flow, in this regime, remains subsonic throughout the shroud and the primary stream is recompressed by a complicated series of shock waves.[14] If the shroud is sufficiently long, the primary and secondary flow can be assumed to be subsonic and uniformly mixed at some downstream location. The ejector characteristics can then be established by a one-dimensional method of analysis similar to that used by Fabri [11] which includes the losses as a result of friction along the shroud wall. However, for the purposes of a unified treatment and ease of calculation, M_{1s} and P_{1s}/P_{0p}, are chosen as the independent variables. On this basis, the ejector-flow characteristics can be found in the form

$$M_{1s} = M_{1s}(P_{1s}/P_{0p}, P_a/P_{0p}) \tag{32}$$

and

$$\frac{W_s}{W_p} = \frac{W_s}{W_p}\left(\frac{P_{0s}}{P_{0p}}, \frac{P_a}{P_{0p}}\right) \tag{33}$$

A particularly useful representation of the overall operating

[13] M. Sirieix, in a recent publication [18], obtained a solution for this flow regime (Region I) by assuming $M_{1s} = 0$ and then employing constant-pressure jet boundaries in his calculations. However, a modification of the theory, which considered the mixing-region thickness near the reattachment point, was necessary to obtain agreement with experimental results.

[14] Termed by Fabri as the "mixed" flow regime.

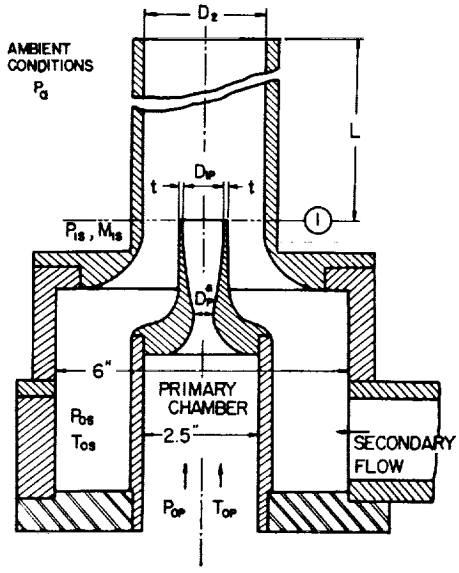

Fig. 10 Experimental ejector configuration

characteristics of an ejector system can be obtained by representing equations (30) and (32) as an ejector "solution surface," Fig. 8. It should be noted that the "break-off curve" defines the transition from the flow regime which is independent of ambient pressure ratio to the regime which is dependent on this ratio. This curve is established when M_{1sl} obtained from equation (30) also satisfies equation (32) for a particular pair of values of P_{1s}/P_{0p} and P_a/P_{0p}. The $(P_a/P_{0p})_s$ value is determined on this curve when P_{1s}/P_{0p} is the corresponding base-pressure ratio.

The steady-state, mass-flow characteristics can also be presented as a three-dimensional "solution surface," Fig. 9; also shown in this figure is a typical "locus of quasi-steady" operating conditions for the ejector starting analysis (where W_s/W_p is now considered as a function of $\zeta = P_{0s}(t)/P_{0p}$).

Calculation of the Starting Characteristics

$W_s/W_p = W_s/W_p(\zeta)$, established from equation (31), may now be used to evaluate numerically the integral in equation (7). The initial condition is that at $t = 0$, the flow ratio is given by

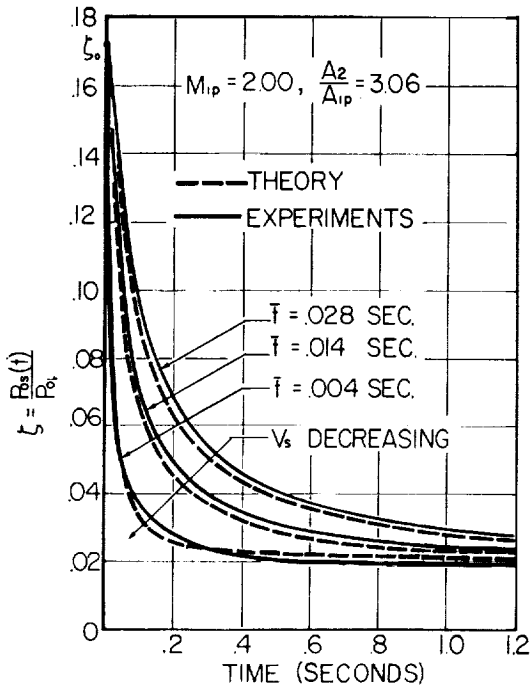

Fig. 11(a) Transient starting characteristics of an ejector system (ζ versus t)

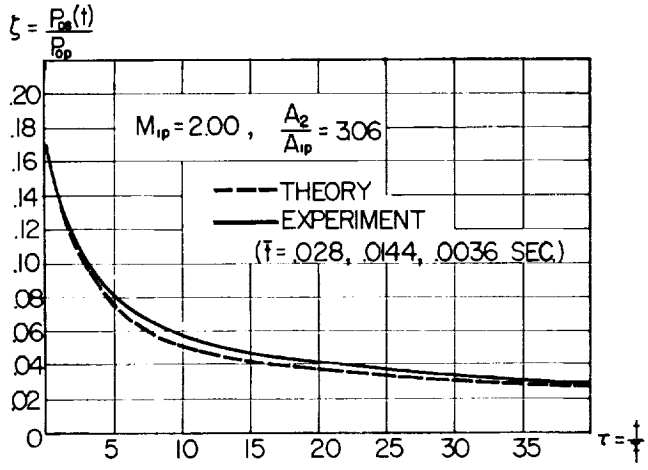

Fig. 11(b) Transient starting characteristics of an ejector system (ζ versus τ)

$$\left[\frac{W_s}{W_p}\right]_{t=0} = \frac{W_s}{W_p}(\zeta_0)$$

This initial condition is justified as a result of the very rapid establishment of the flow fields. It is expedient to define a characteristic time for the starting process as

$$\bar{t} = \left[V_s\left(\frac{P_{0s,0}}{P_{0p}}\right)\Big/ A_{1s}(kg_cRT_{0s,0})^{1/2}I_1(\eta_j,\ \varphi_b = 0,\ C^2_{pa,R})\right] \quad (34)$$

where $C_{pa,R}$ is the reference Crocco number of the primary stream which corresponds to the base-pressure solution, $M_{1sl} = 0$. Equation (7) is now of the form

$$(\tau - \tau_0) = (t/\bar{t} - t_0/\bar{t}) = E(\zeta, \zeta_0) \quad (7a)$$

Theoretical and Experimental Results

The experimental investigation was carried out with a small-scale cold-flow ejector model, Fig. 10. The primary flow was supplied by a compressor with a capacity of 0.8 lb per sec at a pressure level of 100 psia. The secondary flow was supplied either from atmosphere or pressurized tanks.

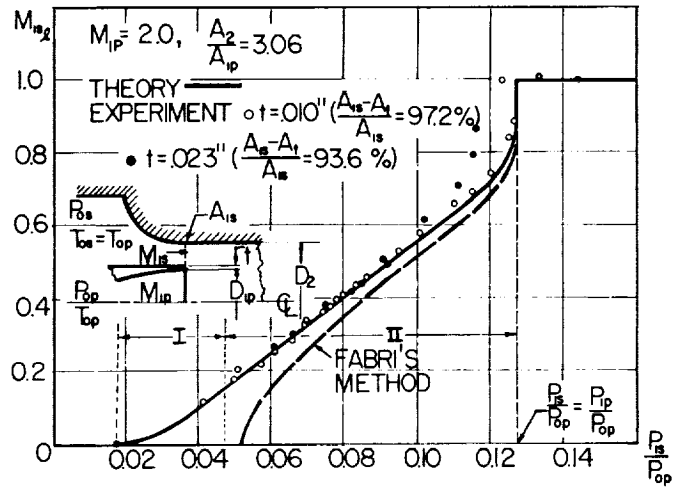

Fig. 12(a) Steady-state ejector characteristics at low ambient pressure ratios (M_{1sl} versus P_{1s}/P_{0p})

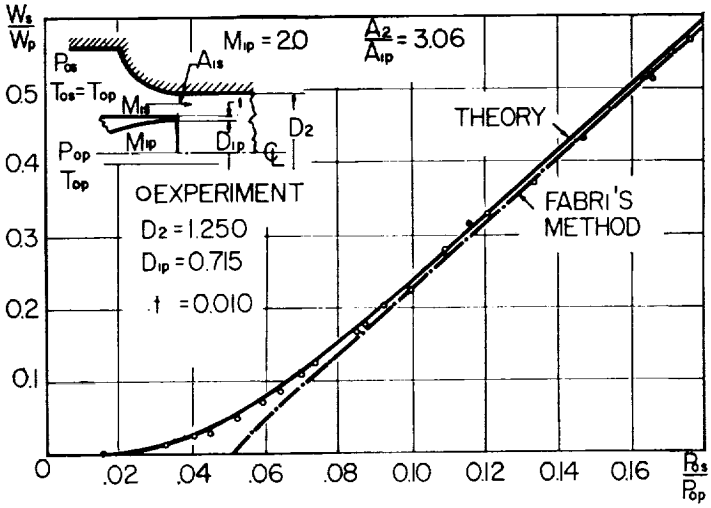

Fig. 12(b) Steady-state, mass-flow characteristics at low ambient pressure ratios (W_s/W_p versus P_{0s}/P_{0p})

For the starting study, the primary flow was established by a quick-opening valve in less than 7 millisec. The secondary chamber was a sealed but yet variable volume. All pertinent pressure measurements were made using unbounded-strain gage transducers and were recorded with an oscillograph. The experimentally determined variation of the secondary stagnation pressure with respect to time, for a constant initial value of P_{0s}/P_{0p} ($t = 0$) and various values of the secondary volume, is presented in Fig. 11(a) for an ejector system with $M_{1p} = 2.0$ and $A_2/A_{1p} = 3.06$. These data can be reduced into a single curve by plotting this variation against a dimensionless time, $\tau = t/\bar{t}$, as shown in Fig. 11(b).

For steady-state operation, the secondary flow was measured with a VDI standard nozzle, and the pressure measurements were made with precision manometers. Steady-state experiments, for an ejector system with $M_{1p} = 2.0$ and $A_2/A_{1p} = 3.06$, were made. The values of the "limiting initial secondary-flow Mach number" (M_{1sl}) were calculated from the experimental pressure data and are presented in Fig. 12(a) for various values of the measured pressure ratio P_{1s}/P_{0p}. The measured secondary mass-flow rate is presented in Fig. 12(b) as a function of the stagnation pressure ratio P_{0s}/P_{0p}; this flow rate was also confirmed by calculations based on the experimental pressure data.

Theoretical calculations, based on the methods of this paper, were made for the ejector system tested. The results of these

calculations are presented in Figs. 11 and 12 for direct comparison with experiments. Also shown in Fig. 12 are the steady-state characteristics of this ejector system which were calculated by Fabri's method [11].

Discussion

It is obvious from the results which have been presented here that the agreement between the present theory and experiments is very good. Although Fabri's analysis gives comparable results for the steady-state analysis, his method cannot be employed for ejector systems with non-constant area shrouds. In addition, Fabri's method cannot be used to predict starting characteristics, since the viscous effects were completely ignored.

It should be mentioned that the scope of this analytical and experimental investigation actually covered three ejector systems [1] ($M_{1p} = 2.0$, $A_2/A_{1p} = 3.06$ and 1.96; $M_{1p} = 1.5$, $A_2/A_{1p} = 4.39$). Good agreement between the theory and experiment was also obtained for the ejector systems which are not reported here.

The present steady-state analysis can be used to study ejector systems with arbitrary shroud shapes if the minimum-area criterion is redefined, and it can also be extended to consider fluids of different compositions.

Acknowledgment

This portion of the work was partially supported by NASA, as part of a broad research program under the Research Grant NsG-13-59 entitled "Basic Flow Mechanism and Heat Transfer in Separated Flows." The authors are grateful to Prof. H. H. Korst, who is project director of this program, for his many valuable discussions and encouragement of this portion of the work.

References

1 A. L. Addy, "On the Steady State and Transient Operating Characteristics of Long Cylindrical Shroud Supersonic Ejectors (With Emphasis on the Viscous Interaction Between the Primary and Secondary Streams)," PhD thesis, Department of Mechanical Engineering, University of Illinois, June, 1963.

2 H. H. Korst, W. L. Chow, and G. W. Zumwalt, "Research on Transonic and Supersonic Flow of a Real Fluid at Abrupt Increases in Cross Section (With Special Consideration of Base Drag Problems)," Final Report, ME-TR-392-5, Engineering Experiment Station, University of Illinois, OSR-TR-60-74, Contract No. AF 18(600)-392.

3 H. H. Korst, ' A Theory for Base Pressures in Transonic and Supersonic Flow," *Journal of Applied Mechanics*, vol. 23, TRANS. ASME, vol. 78, 1956, pp. 593–600.

4 W. L. Chow, "On the Base Pressure Resulting From the Interaction of a Supersonic External Stream With a Sonic or Subsonic Jet," *Journal of the Aero-Space Sciences*, vol. 26, 1959, pp. 176–180.

5 P. Carriere and M. Siriex, "Facteurs d'influence du recollement d'un écoulement supersonique," presented at the 10th International Congress of Applied Mechanics, Stresa, Italy, September, 1960, also Technical Memo 20, ONERA, France, 1961.

6 H. K. Ihrig, Jr., and H. H. Korst, "Quasi-Steady Aspects of the Adjustment of Separated Flow Regions to Transient External Flow," *AIAA Journal*, vol. 1, 1963, pp. 934–937.

7 F. D. Kochendorfer and M. D. Rousso, "Performance Characteristics of Aircraft Cooling Ejectors Having Short Cylindrical Shrouds," NACA RM E51E01, May, 1951.

8 L. Crocco, *One-Dimensional Treatment of Steady Gas Dynamics*, Fundamental of Gas Dynamics, edited by H. W. Emmons, Princeton University Press, Princeton, N. J., vol. 3, 1958, pp. 272–293.

9 J. Fabri, R. Siestrunck, and E. LeGrives, "Etude aérodynamique des trompes supersoniques," *Jahrbuch 1953 der Wissenschaftlichen Gesellschaft für Luftfahrt*, Braunschweig, 1954, vol. 11, pp. 101–110.

10 J. Fabri and R. Siestrunck, "Etude des divers regimes d'ecoulement dans l'enlargissement brusque d'une veine supersonique," *Revue generale des Sciences Appliques*, Brussels, vol. 2, 1955, pp. 229–237.

11 J. Fabri and J. Paulon, "Theory and Experiments on Supersonic Air-to-Air Ejectors," NACA TM 1410, 1958.

12 R. C. German and R. C. Bauer, "Effects of Diffuser Length on the Performance of Ejectors Without Induced Flow," AEDC TN 61-89, August, 1961.

13 R. C. Bauer and R. C. German, "The Effect of Second Throat Geometry on the Performance of Ejectors Without Induced Flow," AEDC TN 61-133, November, 1961.

14 A. H. Shapiro, *The Dynamics and Thermodynamics of the Compressible Fluid Flow*, Ronald Press, New York, N. Y., 1953, vol. 1, pp. 73–87; vol. 2, pp. 676–682.

15 R. J. Golik, "On Dissipative Mechanisms Within Separated Flow Regions (With Special Consideration to Energy Transfer Across Turbulent, Compressible, Pr = 1, Mixing Region)," PhD thesis in Mechanical Engineering, University of Illinois, June, 1962.

16 H. H. Korst, "Auflosung eines ebenen Freistrahlrandes bei Berucksichtigung der Ursprunglichen Grenzschichtstromung," *Csterreicnisches Ingenieur-Archiv*, vol. 3, 1954, also "Compressible Two-Dimensional Jet Mixing at Constant Pressure," ME-TN-392-1, OSR-TN-54-82. University of Illinois, April, 1954, reproduced as OTS collection Pb 132044, Department of Commerce.

17 H. H. Korst and W. L. Chow, "Compressible Non-Isoenergetic Turbulent ($Pr_t = 1$) Jet Mixing Between Two Compressible Streams at Constant Pressure," ME-TN-393-2, Engineering Experiment Station, University of Illinois, Report in preparation for the Research Grant NASA NsG-13-59.

18 M. Sirieix, "Contribution a l'etude des ejecteurs supersoniques," TP No. 32, Association Technique Maritime et Aeronautique, May, 1963.

19 H. Gortler, "Berechnung von Aufgaben der freien Turbulenz auf grund eines neuen Naherungsansatzes," *ZAMM*, vol. 22, 1942, pp. 244–254.

Printed in U. S. A.